

Supporting Information

**A Chiral MOFs Membrane for Enantioselective Amino  
Acid Separation**

Jinhua Xu<sup>a</sup>, Jinyu Zhang<sup>a</sup>, Wenmin Zhang<sup>b</sup>, Shiye Xie<sup>a</sup>, Lan Zhang<sup>a</sup>

<sup>a</sup> Ministry of Education Key Laboratory for Analytical Science of Food Safety and Biology, Fujian Province Key Laboratory of Analysis and Detection Technology for Food Safety, College of Chemistry, Fuzhou University, Fuzhou, Fujian, 350116, China

<sup>b</sup> Department of Chemistry and Biotechnology, Minjiang Teachers College, Fuzhou, Fujian, 350108, China

\* Corresponding authors: Lan Zhang

E-mail addresses: [zlan@fzu.edu.cn](mailto:zlan@fzu.edu.cn)

## Table of Contents

1. Experimental section.....	3
2.1 Chemical reagents .....	3
2.2 Apparatus .....	3
2.3 Synthesis of F-CMOF with various morphology .....	5
2.4 Synthesis of F-CMOF membrane: .....	5
2.5 Chiral molecule permeation test.....	6
2.6 Adsorption Experiments .....	7
2.7 HPLC-UV analysis amino acid enantiomer .....	7
2. Data.....	8
Table S1 Element content of F-CMOF. ....	8
Table S2 Compared with other CMOF membrane. ....	9
Figure S1. (a) Crystal structure diagram of F-CMOF, (b) The cell stacking structure diagram of F-CMOF, (c) Connolly surface plot of Parallel to A & B Axis of F-CMOF, with orifices in blue and F-CMOF skeleton in red.....	10
Figure S2. Mass spectrometry of F-CMOF.....	11
Figure S3. SEM images of F-CMOF. ....	12
Figure S4. High-resolution XPS spectra Cu 2p (a), N 1s (b) and O 1s (c) of F-CMOF.....	13
Figure S5. Adsorption capacity of F-CMOF membrane towards Phe and Trp enantiomers...14	
Reference .....	15

## 1. Experimental section

### 2.1 Chemical reagents

Cupric chloride ( $\text{CuCl}_2$ ), methyl sulfoxide (DMSO), CTAB, (R) -Tryptophan (R-Trp), (S) -Tryptophan (S-Trp), ethanol, (R) -2-Amino-3-phenyl-1-propanol (R-App), (S) -2-Amino-3-phenyl-1-propanol (S-App), R- and S-Aspartic acid (R- and S-Asp), R- and S-histidine (R- and S-His), R- and S-phenylalanine (R- and S-Phe), R- and S-glutamate (R- and S-Glu), R- and S-cystine (R- and S-Cys),  $\gamma$ -Aminopropyl triethoxysilane (APTES), sodium hydroxide (NaOH) and aqueous ammonia (25 wt%) were obtained from Aladdin Reagent Co. Ltd. (Shanghai, China). Where R indicates dextrorotatory (Latin: rectus) and S indicates levorotatory (Latin: sinister).

### 2.2 Apparatus

Transmission electron microscopy (TEM) images were obtained using FEI Tecnai G2 F20 instruments (FEI, USA). SEM images were obtained using a Tungsten Filament SEM3200 (CIQTEK, China) operated at an accelerating voltage of 5-15 kV. Samples were coated with a thin layer of gold (Au) using a sputter coater to improve conductivity and reduce charging effects. Morphological characteristics such as particle size, surface texture, and aggregation state were analyzed from the acquired micrographs.  $\text{N}_2$  sorption-desorption isotherms were recorded on a BSD-660S Analyzer (BeiShiDe, China) at 77 K. Prior to measurement, samples were degassed under vacuum at 120 °C for 12 hours to remove physically adsorbed moisture and gases. The specific surface area was calculated using the Brunauer-Emmett-Teller (BET) method in the relative pressure ( $P/P_0$ ) range of 0.05-0.30. The total pore volume

was determined at  $P/P_0 \approx 0.99$ . Pore size distribution was calculated from the adsorption branch of the nitrogen isotherm using the Barrett-Joyner-Halenda (BJH) method. The analysis was performed using the software provided with the BSD-660S analyzer. The BJH model assumes cylindrical pore geometry and is suitable for mesoporous materials with pore sizes ranging between 2-50 nm. The distribution curve provides insights into the uniformity and hierarchy of the pore structure. Surface areas of materials were calculated using the Brunauer-Emmett-Teller (BET) method. X-ray diffraction (XRD) measurements were conducted with a D/max-2500 diffractometer (Rigaku, Japan) equipped with Cu K $\alpha$  radiation ( $\lambda = 1.5406 \text{ \AA}$ ) operated at 40 kV and 40 mA. The data were collected over a  $2\theta$  range of  $5-50^\circ$  with a scanning rate of  $5^\circ/\text{min}$  and a step size of  $0.02^\circ$ . The samples were finely ground and mounted on a sample holder prior to measurement. Phase identification was performed by comparing the obtained diffraction patterns with reference data from the JCPDS database. Fourier-transform infrared (FTIR) spectroscopy was performed with a Nicolet iS50 (Thermo Fisher, USA). Circular dichroism (CD) spectra were measured with a circular dichroism spectrometer MOS-450 (Bio-Logic, France) at room temperature. Samples were dissolved in deionized water at a concentration of 0.10-0.20 mg/mL. Spectra were collected over a wavelength range of 200-400 nm using a 1 mm path length quartz cuvette. A scanning speed of 100 nm/min and bandwidth of 1.00 nm were used. Baseline correction was performed using the corresponding solvent. Molecular weights were determined using a liquid chromatography-quadrupole time-of-flight tandem mass spectrometer (LC-Q-TOF-MS, G6520B,

Agilent, USA). Thermogravimetric analysis (TGA) was performed using a simultaneous thermal analyzer (STA449F5, STA, Germany). Elemental analysis was obtained using an organic elemental analyzer (Unicube, Germany). Energy-dispersive spectroscopy (EDS) was obtained using octane elect super energy spectrum (EDAX Inc, USA).

### **2.3 Synthesis of F-CMOF with various morphology**

Weigh 204.2 mg of R-Trp (or S-Trp), 134.4 mg of CuCl<sub>2</sub>, 3.6 mg of CTAB, and 40.0 mg of NaOH into 40.0 mL of water. After sonication (100 W) for 1min to dissolve the solids, the mixture was vortexed 3000 rpm/min for 3 min and allowed to settle for 10 min. The resulting slurry was centrifuged at 6000 rpm/min for 1 min, and the supernatant was discarded. The solid was then washed with deionized water and anhydrous ethanol, followed by centrifugation; this washing process was repeated three times. Finally, the solid was dried under vacuum at 60 °C for 2 h to obtain Cu(Trp)-F-CMOF. The chiral flower-like CMOF synthesized using R-Trp was designated as Cu(Trp)-F-RMOF, while the one synthesized using S-Trp was designated as Cu(Trp)-F-SMOF. The CMOF synthesized using RS-Trp was designated as Cu(Trp)-RSMOF.

### **2.4 Synthesis of F-CMOF membrane:**

The membrane was prepared by in-situ fabrication at room temperature between Trp (20.4 mg) and CuCl<sub>2</sub> (0.5 mol/L, 10 mL) under the presence of CTAB (0.4 mg) and NaOH (4.0 mg). First, the PES substrate was horizontally placed into the APTES (v:v, 50%:50%, 10 mL) solution at 50 °C for 2 h. Then, membrane was thoroughly washed

with water and ethanol mixture and then dried at 50 °C. Then the membrane was placed into the CuCl<sub>2</sub> (0.5 mol/L, 10 mL) solution at room temperature for 30 min, and then thoroughly washed with water and ethanol mixture and then dried at 50 °C. Subsequently, the membrane was placed into the 4 mL solution (20.4 mg Trp, 0.4 mg CTAB and 4.0 mg NaOH ) at room temperature for 10 min, and then thoroughly washed with water and ethanol mixture and then dried at 50 °C.

### **2.5 Chiral molecule permeation test**

Chiral separation experiments were performed in a diffusion cell with two chambers. The chiral composite membrane was placed between the chambers with an effective area of 2.25 cm<sup>2</sup>. The aqueous solutions of single enantiomers, i.e., R-Phe, S-Phe, R-Trp and S-Trp in different concentrations, were added to the feed side. All amino acids are used at their isoelectric point without altering the pH. The same volume of pure water was added to the permeate side. Both the feed and permeate sides were stirred continuously using magnetic stirrer equipment. Every 2 hours, 2 mL was taken from the permeate sides and analyzed for an ultra-violet spectrometer to calculate solute flux  $J$  (mmol/m<sup>2</sup>/s) of enantiomers using equation (1).

$$J = \frac{Q}{A.t} \quad (1)$$

where  $Q$  (mmol) is the molar mass of enantiomers penetrated,  $A$  (m<sup>2</sup>) is the effective area of the membrane, and  $t$  (s) is the experimental time.

Similarly, the separation of racemic phenylalanine and tryptophan solution was added to the feed chamber, and the permeate was analyzed by HPLC. The enantiomeric excess was calculated from the peak areas of each enantiomer, namely

$A_R$  (R enantiomer) and  $A_S$  (S enantiomer), using the equation below:

$$ee\% = \frac{A_R - A_S}{A_R + A_S} \times 100 \quad (2)$$

## 2.6 Adsorption Experiments

Adsorption experiments were carried out in a glass bottle. The membrane was placed in 100 mL of an aqueous solution of R-Phe, S-Phe, R-Trp and S-Trp. The solution was stirred continuously, and every 2 h, 2 mL of the solution was taken for UV analysis. The permeated amino acid concentration was calculated by calibration curve, and the adsorption capacity  $Q$  (mg/g) was calculated by equation (3).

$$Q = \frac{(C_i - C_t) \times V}{M} \quad (3)$$

where  $C_i$  (mg/mL) and  $C_t$  (mg/mL) represent the initial and experimental time concentration of amino acid in the solution, respectively,  $V$  (mL) is the solution volume, and  $M$  (g) is the mass of the membrane.

## 2.7 HPLC-UV analysis amino acid enantiomer

Cyclobond I 2000 column : 250 mm×4.6 mm, particle size 5 $\mu$ m, mobile phase acetonitrile ( ACN ) : methanol ( MeOH ) = 50 : 50 ( v / v ), containing 0.1 % DEA / TFA, flow rate 0.8 mL / min, column temperature : 25 °C, UV detection wavelength : chiral tryptophan 280 nm, phenylalanine ( Phe ) at 257 nm.

## 2. Data

**Table S1** Element content of F-CMOF.

Sample	N(%)	C(%)	H(%)	O(%)
F-CMOF	11.06	54.65	4.76	14.93

Note: Combustion artifacts in metal-organic frameworks: MOFs containing transition metals such as Cu are known to exhibit catalytic activity during combustion, which can lead to partial decomposition or charring of the organic components rather than complete oxidation. This can suppress the release of hydrogen as water vapor during CHN analysis, leading to an underestimation of hydrogen content.

**Table S2** Compared with other CMOF membrane.

Membrane	Chiral Ligand	Ee (%)	Flux (mmol/m <sup>2</sup> /s)	Fabrication Method	Ref
Co-MOF	dimethyl pyridine-2,5-dicarboxylate	100	$1.94 \times 10^{-6}$	In-situ on (PANI)- $\alpha$ -Al <sub>2</sub> O <sub>3</sub> substrate	1
Zn-MOF	L-histidine	76	$1.87 \times 10^{-6}$	In-situ on anodic aluminum oxide	2
Cu-MOF	bovine serum albumin	86.55	$4.40 \times 10^{-6}$	MOF-919@BSA embedded in PES	3
Zr-MOF	L-Alanine L-threonine L-histidine	95	$1.25 \times 10^{-6}$	Secondary Growth on $\alpha$ -Al <sub>2</sub> O <sub>3</sub>	4
Cu-MOF	D-(+)-camphoric acid	90	$8.61 \times 10^{-7}$	polydopamine-mediated counter-diffusion polycarbonate	5
Cu-MOF	R-/S-Tryptophan	99.69	$19.85 \times 10^{-6}$	In-situ on PES	This work

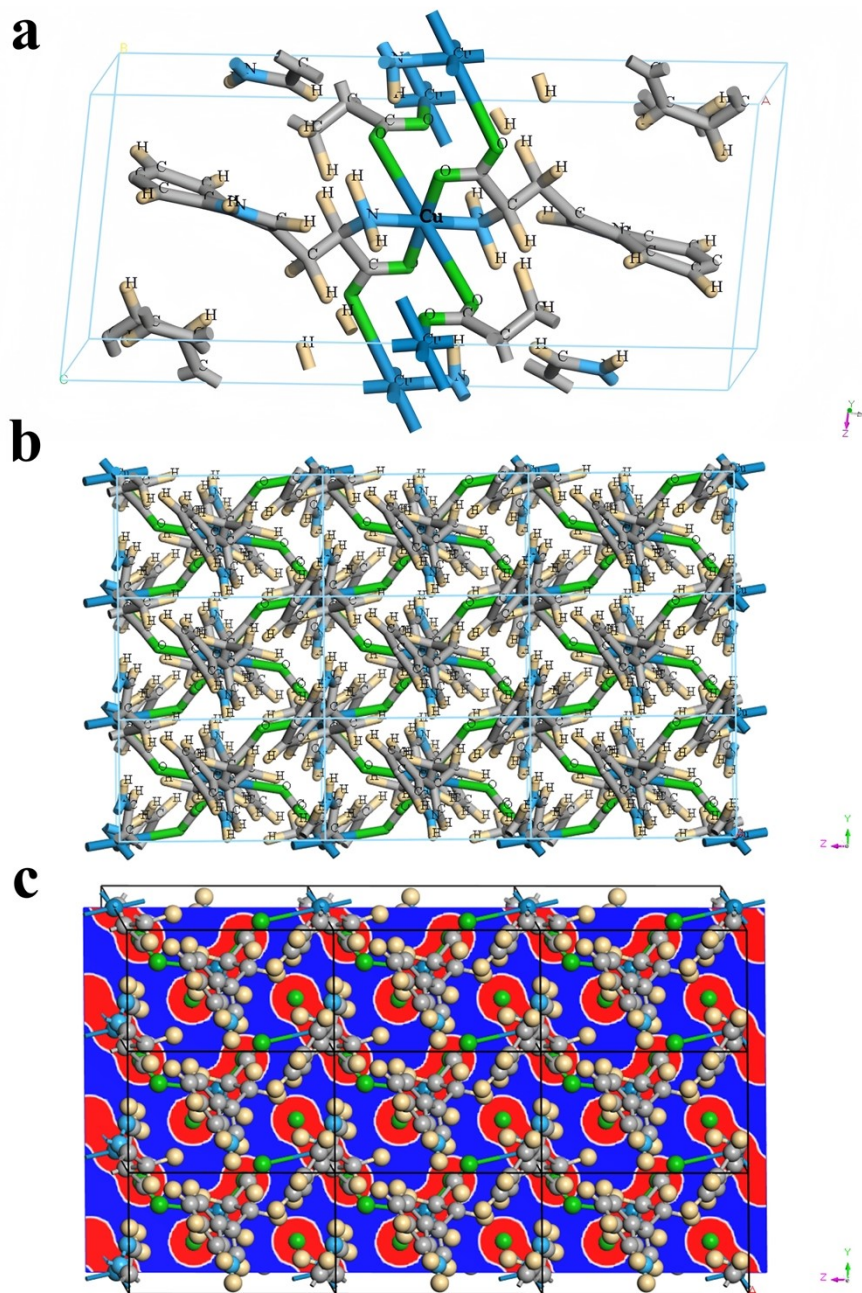


**Figure S1.** (a) Crystal structure diagram of F-CMOF, (b) The cell stacking structure diagram of F-CMOF, (c) Connolly surface plot of Parallel to A & B Axis of F-CMOF, with orifices in blue and F-CMOF skeleton in red.

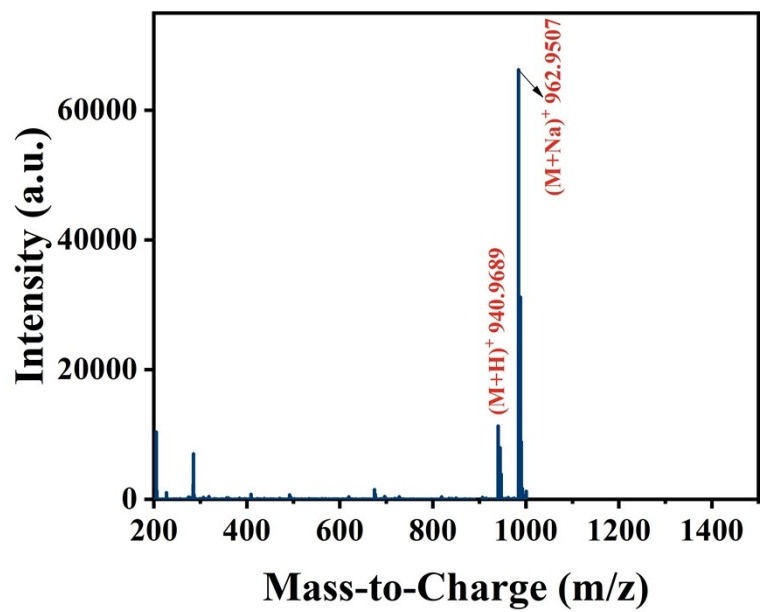


**Figure S2.** Mass spectrometry of F-CMOF.

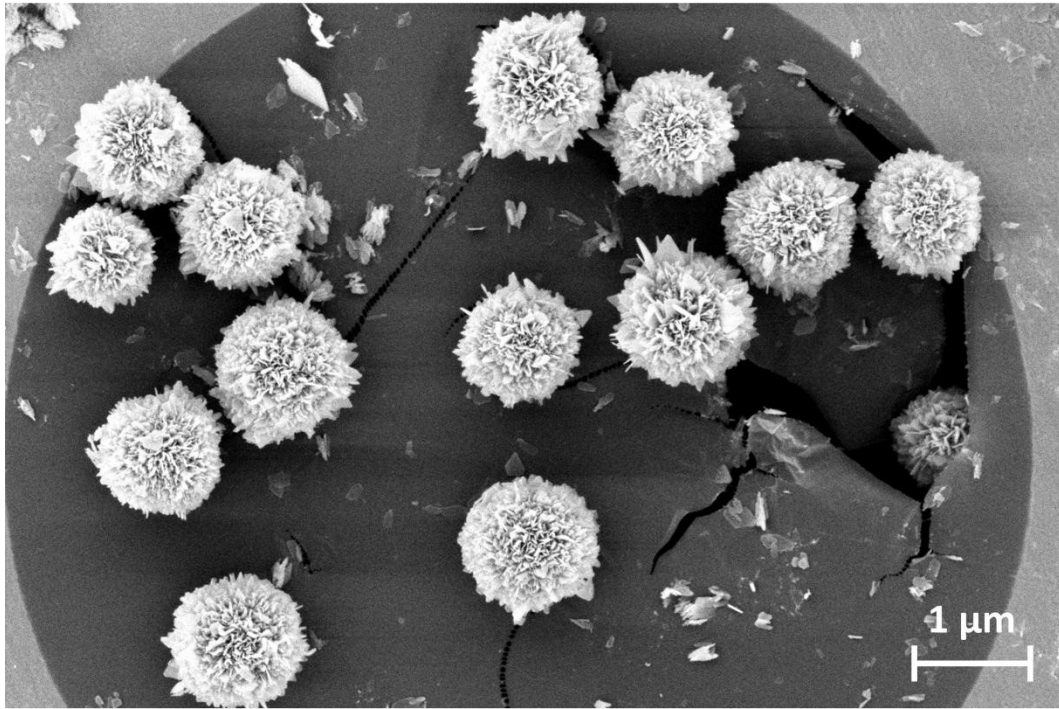


**Figure S3.** SEM images of F-CMOF.

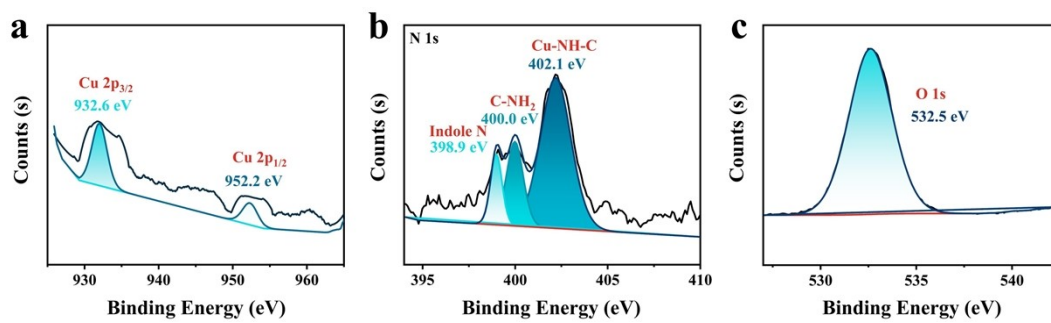


**Figure S4.** High-resolution XPS spectra Cu 2p (a), N 1s (b) and O 1s (c) of F-CMOF.

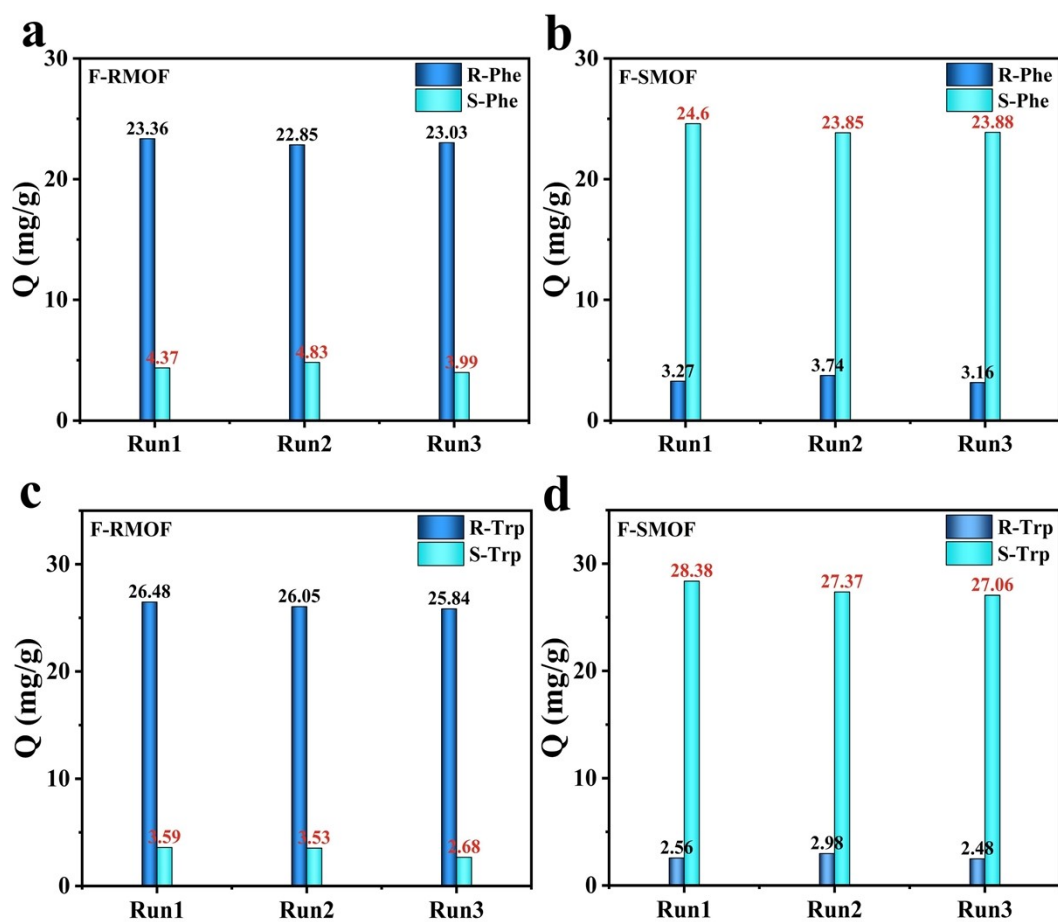


Figure S5. Adsorption capacity of F-CMOF membrane towards Phe and Trp enantiomers.

## Reference

1. B. Li, Y. Feng, D. Zhou, M. Yang, D. Li, S. Zhang, J. Fu and T. Ben, *J. Mater. Chem. A*, 2025, **13**, 8375-8384.
2. J. Y. Chan, H. Zhang, Y. Nolvachai, Y. Hu, H. Zhu, M. Forsyth, Q. Gu, D. E. Hoke, X. Zhang, P. J. Marriot and H. Wang, *Angew. Chem. Int. Ed.*, 2018, **57**, 17130-17134.
3. X. Shang, R. Ji, L. Gao, S. Li, R. Qiu and T. Wang, *J. Membr. Sci.*, 2025, **726**, 124057.
4. T. Chen, H. Li, X. Shi, J. Imbrogno and D. Zhao, *J. Am. Chem. Soc.*, 2024, **146**, 14433-14438.
5. M. Chen, X. Li, J. Li, C. Liu, A. Yu and S. Zhang, *Sep Purif Technol*, 2024, **331**, 125704.